ISSN 1061-933X, Colloid Journal, 2024. © The Author(s), 2024. This article is an open access publication.

Kinetic Regularities of the Synthesis of Silica Nanoparticles by Heterogeneous Hydrolysis of Tetraethoxysilane Using *L*-Arginine as a Catalyst

V. M. Masalov[a], N. S. Sukhinina[a], D. N. Sovyk[b, *], V. G. Ralchenko[b], and G. A. Emel'chenko[a]

[a] *Osipyan Institute of Solid State Physics, Russian Academy of Sciences, Chernogolovka, Moscow oblast, 142432 Russia*

[b] *Prokhorov Institute of General Physics, Russian Academy of Sciences, Moscow, 119991 Russia*

**e-mail: sovyk@inbox.ru*

Received November 23, 2023; revised December 5, 2023; accepted December 6, 2023

Abstract—The kinetics of the synthesis of silica nanoparticles (<50 nm) has been studied under the conditions of heterogeneous hydrolysis of tetraethoxysilane (TEOS) using *L*-arginine as an alkaline catalyst. The rates of silica formation have been determined in a temperature range of 10–95°C at catalyst concentrations of 6–150 mM. It has been shown that the activation energy of the process depends on catalyst concentration and varies in a range of 21.5–13.9 kJ/mol, while decreasing linearly with increasing concentration of *L*-arginine in the system. The criterion of maintaining the monodispersity has been estimated for SiO_2 particles being grown "onto seeds." The density of submicron-sized silica particles has been experimentally determined as depending on the annealing temperature. Within a temperature range of 200–1000°C, the particle density varies from 2.04 to 2.20 g/cm^3.

Keywords: amorphous silica, nanospheres, heterogeneous hydrolysis of tetraethoxysilane, colloids, synthesis kinetics

DOI: 10.1134/S1061933X23601257

INTRODUCTION

Nano- and microparticles of amorphous silica are used in catalysis [1, 2], chromatography [3], optics [4], finishing polishing [5, 6], and other fields of engineering. The possibility to vary the porosity of the particles and to functionalize their surface, as well as the biocompatibility of silica, open broad prospects for their use in biology and medicine [7–10]. Ordered three-dimensional structures formed by spherical silica particles are widely applied as model systems for studying molecular diffusion in nanopores [11–14] and as templates for creating ordered inverted polymer- [15, 16], mesoporous carbon- [17, 18] and diamond-based [19, 20] materials.

In 1956, Kolbe was the first to report the preparation of spherical silica particles by tetraethoxysilane (TEOS) hydrolysis in a water-alcohol solution in the presence of ammonia as an alkaline catalyst [21]. In 1968, Stöber, Fink, and Bohn improved this process and showed that it was possible to obtain particles with sizes from 50 nm to 2 μm, an almost ideal spherical shape, and a high monodispersity [22]. Later, it was shown that silica particles could be step-by-step grown in a controllable manner to preliminarily preset sizes by using them as seeds and adding calculated amounts of TEOS to a system [23–25]. Up to the present, various versions of the Stöber method have remained to be the main technique for the synthesis of monodisperse silica particles due to its simplicity and the feasibility to produce particles with a relatively narrow size distribution within a wide range of their diameters (from ~100 to ~3000 nm) [23–30].

The main limitation for the Stöber process is the difficulty to achieve a high monodispersity for particles with sizes smaller than 100 nm. In 2006, Yokoi et al. [31] and Davis et al. [32] proposed a method for producing spherical silica nanoparticles by hydrolyzing TEOS under weakly alkaline conditions (pH 9–10) in an emulsion system containing TEOS; water; and an amino acid, *L*-lysine. The obtained silica particles had diameters of 10–20 nm and a high monodispersity, which was unattainable when particles were grown by the Stöber method.

Hartlen et al. [33] showed that, using the method of heterogeneous hydrolysis of TEOS in the presence of an amino acid (*L*-arginine) as an alkaline catalyst, the sizes of particles could be varied by their growth in the same medium, while maintaining a high monodispersity. Moreover, the authors revealed that these particles could be used as seeds in the processes of the step-by-step growth by the well-studied Stöber method. This made it possible to combine the advantages of both

procedures and obtain particles in a wide range of sizes (from a few tens of nanometers to several microns in diameter) at a high degree of uniformity (<5%).

In spite of the fact that much efforts have, recently, been made in the field of studying the physicochemical processes that accompany the preparation of silica particles by heterogeneous hydrolysis of TEOS in the presence of amino acids, some aspects remain to be additionally studied. In particular, there is a lack of data on the kinetics and mechanism of the formation of colloidal silica particles. In this article, we report the results of studying the kinetics of silica synthesis under the conditions of heterogeneous hydrolysis of TEOS using *L*-arginine as an alkaline catalyst. The obtained experimental data on the rate of TEOS hydrolysis and condensation of its products have been used to calculate the activation energies of the process at different concentrations of *L*-arginine in the system. The article presents the results of estimating the conditions for maintaining the monodispersity of particles being grown, as well as the results of studying variations in the density and porosity of particles during their thermal treatment.

EXPERIMENTAL

Tetraethoxysilane (TEOS, 98%) was preliminarily purified by rectification. *L*-Arginine (99%, Panreac) was used as received. Deionized water (~18 MΩ/cm) was obtained with an Akvilon D-301 deionizer.

Kinetics of silica formation was studied at the total volume of a reaction mixture equal to 300 mL. *L*-Arginine (6–150 mM) was added to deionized water (250 mL), and the mixture was thoroughly stirred on a Heidolph MR MIX-D magnetic stirrer combined with an Elmi TW-2.02 water thermostat until the amino acid was dissolved. The solution was heated to a specified temperature, and TEOS (50 mL) preheated to the same temperature was added. The solution temperature was maintained constant at an accuracy of ±0.1°C within a range of 10–95°C for the entire time interval of the synthesis. In all experiments, the rotation rate of the magnetic stirrer (50 × 8 mm) was maintained constant and equal to 600 rpm to obtain an oil-in-water emulsion. In all experiments, the geometry of the reactor was the same to ensure the reproducibility of the sizes of TEOS droplets in the aqueous medium and the same area of the TEOS–aqueous *L*-arginine solution interface during experiments performed at the same temperature. In the course of the synthesis, samples of the colloidal suspension were taken to determine the weight concentration of SiO_2 particles and to perform electron microscopic examinations. The weight concentration of silica in the aqueous phase of the reaction mixture was determined from the ratio of the weight of silica particles, after they were dried and annealed at 600°C, to the total weight of a suspension sample. The sizes and morphology of the particles were investigated using a Zeiss Supra 50 VP scanning electron microscope. The size of the resulting silica particles varied within a range of 8–45 nm depending on the synthesis conditions.

To study the density of SiO_2 particles, they were grown by the multistep synthesis in the TEOS–aqueous *L*-arginine solution (2 mM) system. For this purpose, a calculated amount of SiO_2 seeds was dispersed in an aqueous *L*-arginine solution using a magnetic stirrer, and a calculated amount of TEOS was added. The seeds were grown at 60°C under continuous stirring at a magnetic stirrer rotation rate of 200–300 rpm, which ensured the continuity of the interface. After colloidal SiO_2 particles had grown to a size of ~300 nm, the suspension was placed into a vessel, in which the particles were subjected to spontaneous sedimentation. The obtained sediment was dried and annealed for 24 h at temperatures of 200–1000°C. The density and porosity of the particles were studied by the method of hydrostatic weighing [34].

RESULTS AND DISCUSSION

Silica synthesis by TEOS hydrolysis includes two main stages: hydrolysis up to the formation of silicic acid followed by polycondensation of its monomers. Schematically, this process may be represented by three main reactions:

Sequential hydrolysis of TEOS:

$$\begin{gathered}(C_2H_5O)_3{\equiv}Si{-}(OC_2H_5) + H_2O \\ \rightarrow (C_2H_5O)_3{\equiv}Si{-}(OH) + C_2H_5OH \\ \rightarrow (C_2H_5O)_2{=}Si{=}(OH)_2 \ldots \\ \rightarrow \ldots(C_2H_5O){-}Si{\equiv}(OH)_3 \ldots \rightarrow \ldots\ Si(OH)_4,\end{gathered} \quad (1)$$

condensation accompanied by release of water:

$$\equiv Si{-}(OH) + (HO){-}Si{\equiv} \rightarrow \equiv Si{-}O{-}Si{\equiv} + H_2O, \quad (2)$$

and condensation accompanied by release of alcohol:

$$\begin{gathered}\equiv Si{-}(OC_2H_5) + (HO){-}Si{\equiv} \\ \rightarrow \equiv Si{-}O{-}Si{\equiv} + C_2H_5OH.\end{gathered} \quad (3)$$

The overall scheme of the hydrolysis–condensation process may be expressed as follows:

$$Si(C_2H_5O)_4 + 2H_2O \rightarrow SiO_2 + 4C_2H_5OH. \quad (4)$$

TEOS hydrolysis occurs at the TEOS–aqueous *L*-arginine solution interface, and, as well as for other heterogeneous reactions, its rate depends on the interface area. The heterogeneous hydrolysis of TEOS yields a water-soluble form of silica, i.e. silicic acid, $Si(OH)_4$ (1), while polycondensation reactions (2), (3) may occur both under homogeneous conditions in the bulk of an aqueous solution (via the interaction of silicic acid molecules with each other) and by the heterogeneous mechanism on the surface of growing particles via the attachment of silicic acid molecules (silica monomers) from the solution [35, 36].

The homogeneous condensation in the aqueous phase of the system yields dimers, trimers, and larger polymeric forms of SiO_2, which can grow to the sizes of insoluble silica seed particles. These particles may be attached to the previously formed growing particles or form new ones via the aggregation mechanism [23]. In view of the complex character of the hydrolysis–polycondensation process, which may involve both heterogeneous and homogeneous reactions, we estimated the rate of the overall process of silica synthesis (4) by studying the dependences of the rate of its formation on *L*-arginine concentration and the synthesis temperature.

Commonly, the rate of a heterogeneous chemical reaction is understood as a variation in the amount (concentration) of interacting substances per unit time related to unit surface area of an interface. When liquid phases are stirred in the emulsion regime, the area of an interface between two liquid phases cannot be determined. Therefore, we estimated the overall rate of the synthesis process by measuring the weight concentration of silica in unit volume of the aqueous phase per unit time. In our case, the observed average process rate is equal to variation in SiO_2 concentration per unit time, while the true process rate is equal to the derivative of current weight concentration C_{SiO_2} of silica with respect to time τ:

$$w = \frac{\Delta C_{SiO_2}}{\Delta \tau} = \frac{dC_{SiO_2}}{d\tau}.$$

Figure 1 presents the experimental dependences of SiO_2 concentration on the time of the heterogeneous hydrolysis of TEOS in two regimes of stirring the reaction mixture, i.e., with the preserved continuity of the TEOS–water interface (curve *1*) and under the emulsion conditions of stirring (curve *2*). Reaction temperature was 60°C, *L*-arginine concentration was 6 mM, aqueous solution volume was 250 mL, and TEOS volume was 50 mL. At TEOS conversion $\alpha = 1$, this corresponded to maximum concentration $[SiO_2] = 0.76$ M (horizontal dashed line in Fig. 1). The emulsion regime of stirring the reaction mixture is preferable because of the higher yield of silica.

The plots in Fig. 1 show that, at the initial stage of the synthesis up to TEOS conversion of ~0.5, variation in silica concentration is linear:

$$C_{SiO_2} = k\tau,$$

where k is the reaction rate constant.

That is, at the initial stage, the reaction rate remains unchanged with time and is independent of the concentrations of the reagents. In other words, the heterogeneous hydrolysis of TEOS followed by the condensation of the hydrolysis products (overall scheme (4)) is a process that corresponds to a zero-order reaction (with respect to TEOS), and the kinetic equation has the following form:

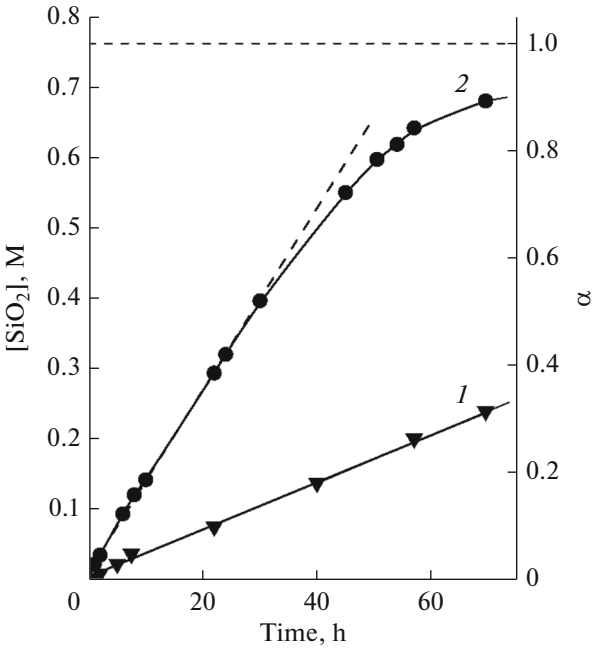

Fig. 1. Variations in silica concentration during TEOS hydrolysis at a temperature of 60°C, *L*-arginine concentration of 6 mM, and different intensities of reaction mixture stirring. Stirrer rotation rates are (*1*) 200 and (*2*) 600 rpm. The right ordinate axis represents TEOS conversion.

$$w = kC_{SiO_2}^{x},$$

where $x = 0$.

In this case, the rate of reaction (4) corresponds to the rate constant of the overall process:

$$w = k.$$

As TEOS is consumed, its amount and the size "droplets" distributed in the aqueous phase of the system decrease. A reduction in the area of the interface between the two immiscible phases leads to a deviation of the dependence from the straight line up to reaching a plateau. The value of the plateau corresponds to the maximum silica concentration that can be obtained proceeding from the water and TEOS volumes used in the reaction (Fig. 1, curve *2*).

Figure 2 shows experimental dependences illustrating the growth of silica concentration with time for reactions performed at different temperatures and *L*-arginine concentrations, with other conditions, including initial volumes of the reagents, reactor geometry, sizes of the magnetic anchor, and its rotation rate, being equal.

Only the rectilinear segments of the kinetic curves were used in the subsequent calculations of the rates of SiO_2 formation. The process rates are numerically equal to their slopes. Figure 3 presents the exponential temperature dependences of the rate of silica synthesis within a range of 10–95°C for different *L*-arginine concentrations (6–150 mM).

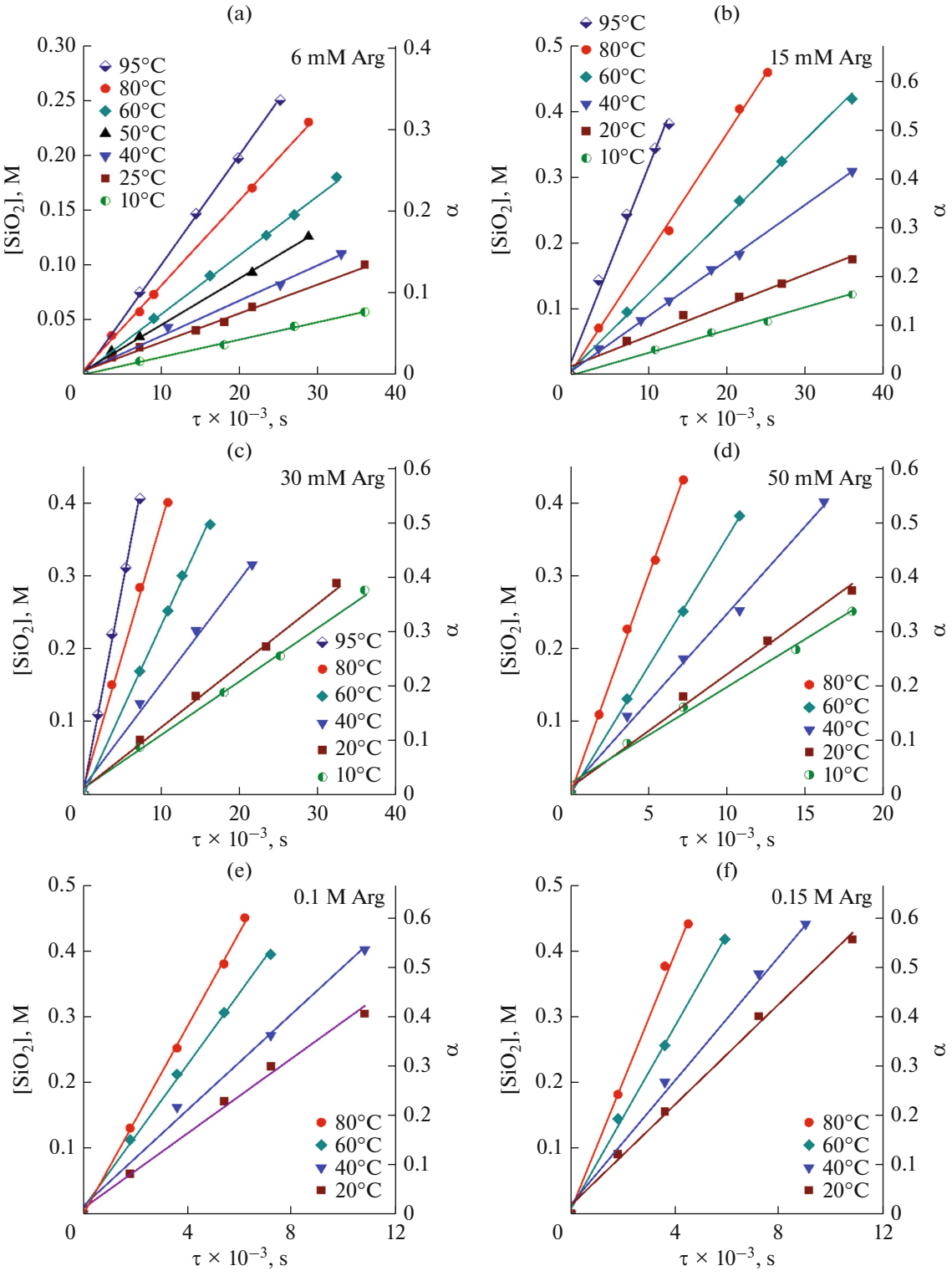

Fig. 2. Kinetic straight lines for heterogeneous hydrolysis–condensation of TEOS at different temperatures and *L*-arginine concentrations.

For *L*-arginine concentrations in the reaction mixture of 6, 15, 30, and 50 mM, elevation of the temperature from 20 to 80°C increases the rate of SiO_2 formation by ~4 times. At higher catalyst concentrations (100 and 150 mM), the effect of temperature on the process rate is somewhat weaker, and the change in the

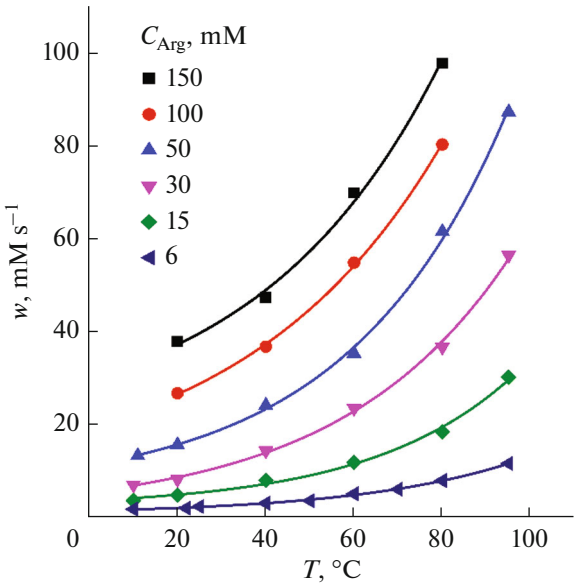

Fig. 3. Temperature dependences of SiO_2 formation rate at different *L*-arginine concentrations.

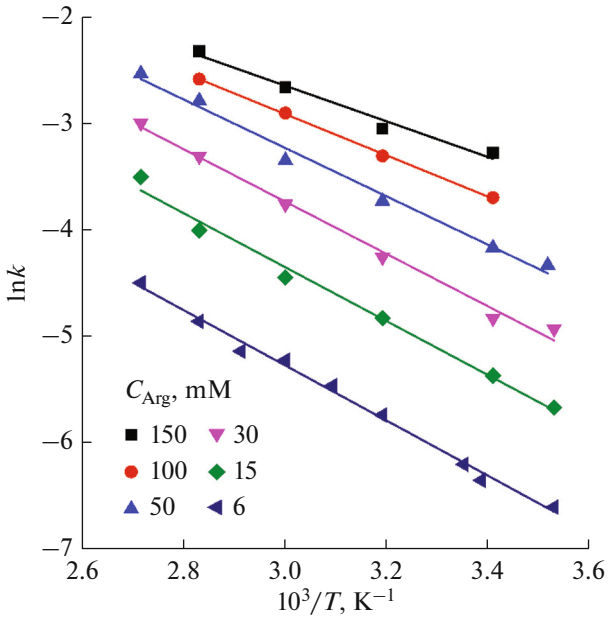

Fig. 4. Temperature dependences of process rate constant at different concentrations of *L*-arginine as a catalyst.

process rate within the same temperature range appears to be 3 and 2.5 times, respectively (see Table 1).

In the $\ln k$–$1/T$ coordinates, the temperature dependences of the process rate constants are adequately described by straight lines (Fig. 4), thereby making it possible to calculate the activation energy of the process at each *L*-arginine concentration by the Arrhenius equation:

$$\ln k = \ln A - E_a/RT,$$

where k is the reaction rate constant, A is a constant, E_a is the activation energy, R is the gas constant, and T is the absolute temperature. The slope of each straight line is equal to $\tan\alpha = -E_a/R$.

Figure 5 presents the dependence of the activation energy on catalyst (*L*-arginine) concentration in the system. Within *L*-arginine concentration range of 6–150 mM, the activation energy of silica synthesis varies from 21.5 to 13.9 kJ/mol and is adequately described by the following equation:

$$E_a = 21.75–54.04[\text{Arg}].$$

The author of [24] has estimated the activation energy of the synthesis of silica particles via homogeneous hydrolysis of TEOS in a water–alcohol solution in the presence of ammonium ions as $E_a = 27$ kJ/mol. When studying the kinetics of TEOS hydrolysis–condensation under the conditions of the homogeneous hydrolysis in a water–alcohol solution in the presence of ammonium ions, the authors of [37] found that the activation energies of hydrolysis and condensation were 25.2 and 33.2 kJ/mol. The values of the activation energy that we obtained for silica synthesis via heterogeneous hydrolysis of TEOS at *L*-arginine concentrations used to prepare monodisperse SiO_2 nanoparticles (7.5 mM [33]) appeared to be close (~21 kJ/mol).

Figure 6a presents a SEM micrograph of silica nanoparticles obtained by heterogeneous hydrolysis of TEOS in the presence of *L*-arginine as a catalyst. Arginine concentration in the aqueous solution was 7.5 mM; volumes of water and TEOS were 500 and 110 mL, respectively; synthesis temperature was 90°C; and magnetic stirrer rotation at a rate of 500 rpm provided the emulsion regime of stirring the two-component system. Synthesis duration was 5 h. Resulting silica particles 42.9 ± 2.5 nm in diameter (Fig. 6a) were used as seeds for subsequent growth. For this purpose, a part of the colloidal suspension was dispersed in an aqueous *L*-arginine solution (2 mM), while the growth under the conditions of heterogeneous TEOS hydrolysis was carried out in milder conditions: reac-

Table 1. Rates w (mM/s) of silica formation process at different *L*-arginine concentrations C_{Arg} and temperatures T

T, °C	C_{Arg}, mM					
	6	15	30	50	100	150
10	1.59	3.45	6.79	13.11		
20	1.8	4.66	7.97	15.45	26.52	37.6
40	2.88	7.8	14.16	23.92	36.52	47.14
60	4.9	11.71	23.27	35.05	54.61	69.6
80	7.75	18.18	36.44	61.27	80.04	97.47
95	11.4	29.98	56.2	87		

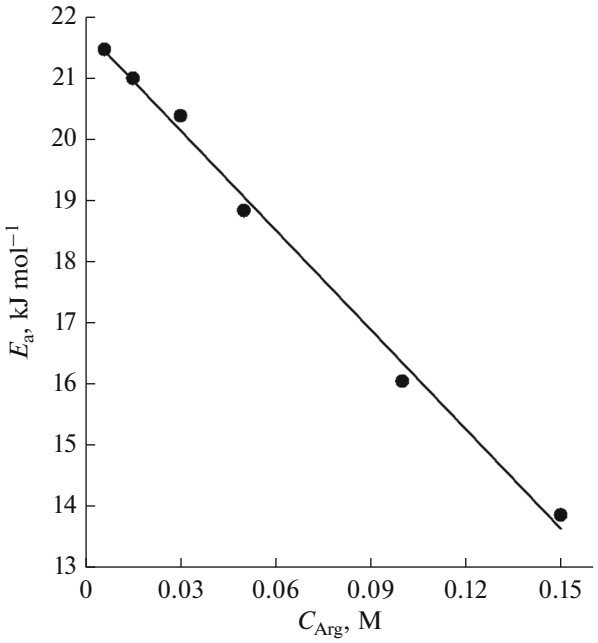

Fig. 5. Dependence of process activation energy on *L*-arginine concentration.

tion temperature was 60°C, while stirrer rotation rate of ~200 rpm corresponded to the condition of "preserved continuity of interface between the liquid phases." Figure 6b shows the SEM micrograph of SiO_2 particles that have reached a diameter of 132.7 ± 2.1 nm. It is seen that the particles are rather monodisperse. The surface of particles obtained by this method is mainly "rough" (see inset in Fig. 6b) in contrast to the "smooth" surface of traditional Stöber particles. This difference is due to the fact that, in the course of the heterogeneous growth, the concentration of dissolved silica ($Si(OH)_4$) remains preserved during the entire synthesis, while, in the case of the homogeneous step-by-step growth of particles via the modified Stöber methods, the concentration of the dissolved silica at the end of each growth step decreases to values, at which the growth proceeds primarily due to the attachment of small SiO_2 nanoparticles and $Si(OH)_4$ monomers to a growing surface.

The monodispersity of silica particles obtained via the growth of seed particles is, to a high extent, predetermined by the relation between the total surface area of seeds and the rate of silica formation in a system. Seemingly, upon the aggregative growth of seed particles, the rate of heterogeneous condensation of hydroxides on their surface and the surface of primary particles being formed is limited. When the ability of utilizing the formed primary particles by the accessible surface of seeds is exceeded, secondary nucleation of new growing particles begins, thus distorting the size monodispersity of the particles. The following experiments were performed to assess the criterion for maintaining the monodispersity. Monodisperse silica particles ~200 nm in diameter were used as seeds. Their different specified amounts were dispersed in an aqueous *L*-arginine solution (2 mM). These seed particles were grown at a controlled rate of silica formation in the system. The monodispersity of the growing particles was monitored by scanning microscopy. As numerical criterion K [g/(h cm^2)], the ratio between silica formation rate w (g/h) and surface area S (cm^2) of seed particles $K = w/S$ was used. Figure 7 illustrates the SEM micrographs of silica particles obtained by growing seeds at $K = 2.13 \times 10^{-6}$ g/(h cm^2) (Fig. 7a) and $K = 2.11 \times 10^{-8}$ g/(h cm^2) (Fig. 7b). The studies have shown that, to maintain the monodispersity of silica particles grown on seeds, synthesis conditions must ensure that the values of K are no higher than ~3.5×10^{-8} g/(h cm^2).

The density and porosity of the grown silica particles were studied by hydrostatic weighing. Figure 8 presents the density of SiO_2 particles 300 nm in diameter as a function of the temperature of their thermal treatment for 24 h within a temperature range of 200–1000°C.

As can be seen in the plot, the particle density varies from 2.04 to 2.20 g/cm^3. The initial density of silica particles obtained by the heterogeneous synthesis in the presence of *L*-arginine exceeds the density of particles obtained by the traditional Stöber method (1.6–1.8 g/cm^3) [23, 26, 38]. Porosity (P) of the particles can be calculated as $P = 1 - \rho_p/\rho_{SiO_2}$, where ρ_p is the particle density and ρ_{SiO_2} is the density of amorphous silica (2.22 g/cm^3). The porosity of initial particles is ~10 vol %. The residual porosity of particles annealed at 1000°C is ~1.2 vol %.

CONCLUSIONS

The kinetics of the synthesis of colloidal silica nanoparticles has been studied under the conditions of heterogeneous hydrolysis of TEOS using *L*-arginine as an alkaline catalyst. The rates of silica formation process have for the first time been determined within a temperature range of 10–95°C at catalyst concentrations of 6–150 mM. The activation energy of silica synthesis has been studied as depending on catalyst concentration. The process activation energy has been shown to linearly decrease in a range of 21.5–13.9 kJ/mol with a rise in *L*-arginine concentration in the system. The criterion for maintaining the monodispersity of SiO_2 particles has for the first time been determined when growing them "onto a seed." The synthesis conditions under which the values of K do not exceed ~3.5×10^{-8} g/(h cm^2) must be maintained to ensure the monodispersity of the particles. A dependence of density on annealing temperature has been experimentally found for submicron silica particles obtained under the conditions of heterogeneous

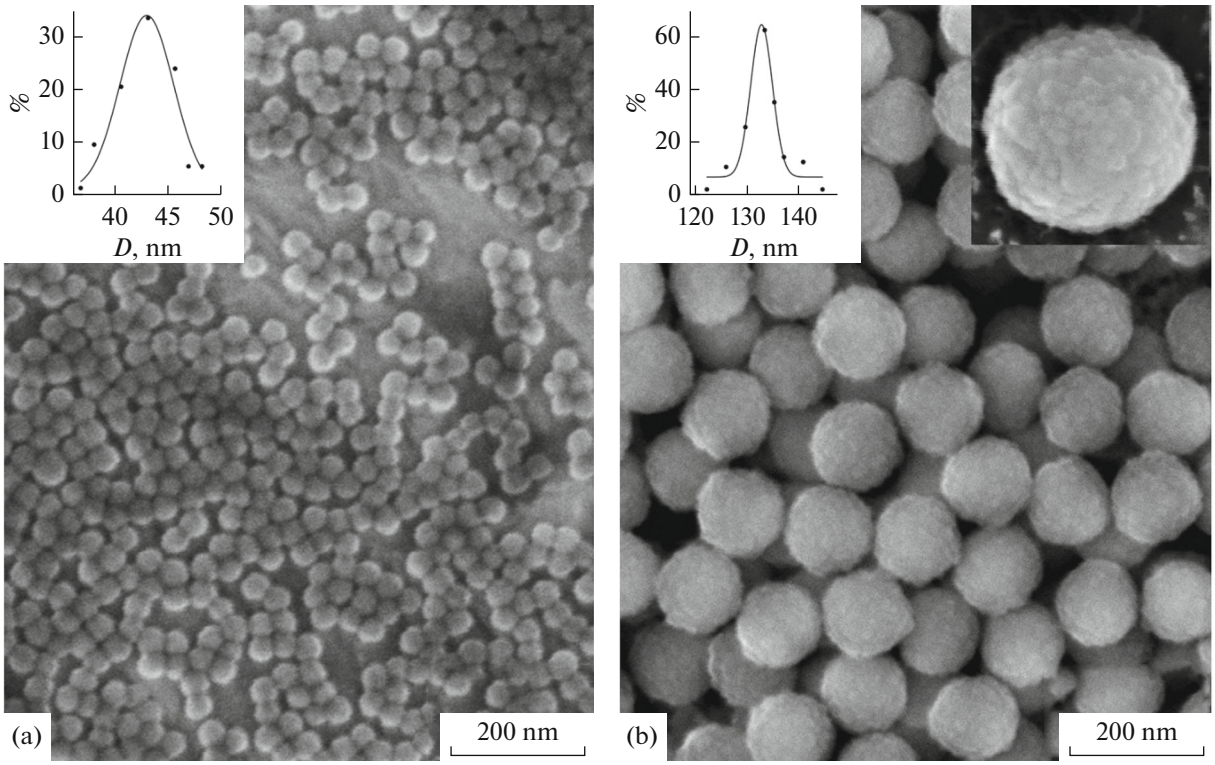

Fig. 6. Silica particles obtained by heterogeneous hydrolysis of TEOS in the presence of *L*-arginine. (b) Silica particles with $D = 132.7 \pm 2.1$ nm resulting from growth of (a) particles with diameter $D = 42.9 \pm 2.5$ nm. Insets show normal particle size distributions.

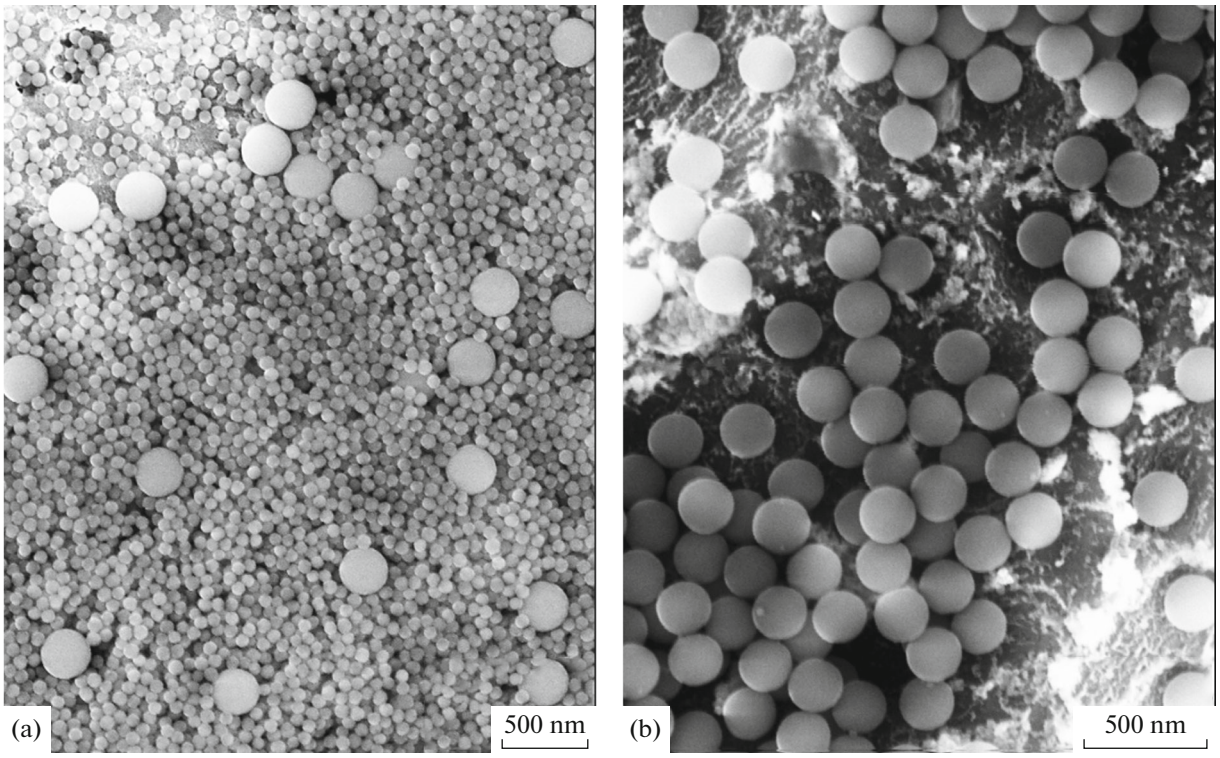

Fig. 7. SEM micrographs of SiO_2 particles obtained by seed growth: (a) bimodal particle size distribution and (b) monodisperse particles.

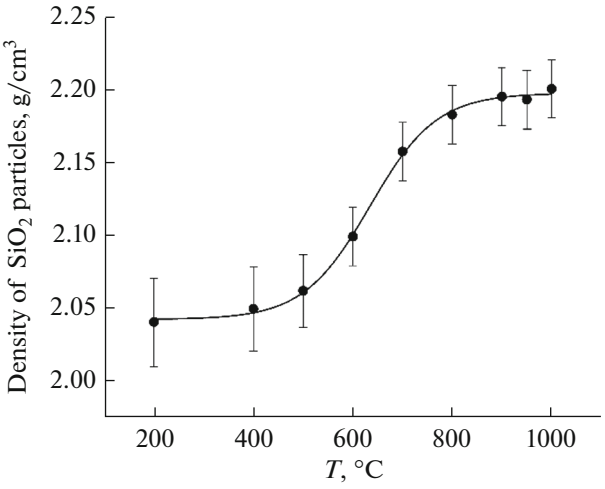

Fig. 8. Dependence of density on annealing temperature for silica particles ~300 nm in diameter obtained via heterogeneous hydrolysis of TEOS in the presence of *L*-arginine. Annealing duration was 24 h.

hydrolysis of TEOS using *L*-arginine as a catalyst. Within a temperature range of 200–1000°C, the particle density varies from 2.04 to 2.20 g/cm^3. Therewith, the total porosity of the particles decreases from 10 to 1.2 vol %. The data obtained on the kinetics of silica formation in the course of heterogeneous hydrolysis of TEOS followed by the polycondensation of silicic acid in the presence of *L*-arginine contribute to the study of the physicochemical foundations of the synthesis and the formation mechanism of nanosized and submicron monodisperse silica nanoparticles. Such particles will be in demand when creating photonic crystals and porous matrices to be used in catalysis, chromatography, biomedicine, etc.

FUNDING

This work was supported by the Russian Science Foundation (project no. 21-12-00403).

CONFLICT OF INTEREST

The authors of this work declare that they have no conflicts of interest.

OPEN ACCESS

REFERENCES

1. Korach, L., Czaja, K., and Kovaleva, N.Y., Sol–gel material as a support of organometallic catalyst for ethylene polymerization, *Eur. Polym. J.*, 2008, vol. 44, no. 3, pp. 889–903. https://doi.org/10.1016/j.eurpolymj.2007.11.037
2. Li, L., Ewing, C.S., Abdelgaid, M., et al., Binding of CO and O on low-symmetry Pt clusters supported on amorphous silica, *J. Phys. Chem. C*, 2021, vol. 125, no. 25, pp. 13780–13787. https://doi.org/10.1021/acs.jpcc.1c01452
3. Tikhomirova, T.I. and Nesterenko, P.N., Specific features of complexation on the surface of modified silica sorbents: Sorption and complexation chromatography of metals, *Russ. J. Coord. Chem.*, 2022, vol. 48, no. 10, pp. 631–640. https://doi.org/10.1134/S1070328422100074
4. Chen, Y., Li, L., Xu, Q., et al., Recent advances in opal/inverted opal photonic crystal photocatalysts, *Sol. RRL*, 2021, vol. 5, no. 6, p. 2000541. https://doi.org/10.1002/solr.202000541
5. Moon, B.-S., Hwang, H.-S., and Park, J.-G., Influences of organic additive molecular weight in colloidal-silica-based slurry on final polishing characteristics of silicon wafer, *J. Electrochem. Soc.*, 2012, vol. 159, no. 2, pp. H107–H111. https://doi.org/10.1149/2.032202jes
6. Bae, J.-Y., Han, M.-H., Lee, S.-J., et al., Silicon wafer CMP slurry using a hydrolysis reaction accelerator with an amine functional group remarkably enhances polishing rate, *Nanomaterials*, 2022, vol. 12, no. 21, p. 3893. https://doi.org/10.3390/nano12213893
7. Ding, Y., Xiao, Z., Chen, F., et al., A mesoporous silica nanocarrier pesticide delivery system for loading acetamiprid: Effectively manage aphids and reduce plant pesticide residue, *Sci. Total Environ.*, 2023, vol. 863, p. 160900. https://doi.org/10.1016/j.scitotenv.2022.160900
8. Zhang, Z., Li, W., Chang, D., et al., A combination therapy for androgenic alopecia based on quercetin and zinc/copper dual-doped mesoporous silica nanocomposite microneedle patch, *Bioact. Mater.*, 2023, vol. 24, pp. 81–95. https://doi.org/10.1016/j.bioactmat.2022.12.007
9. Wang, H., Chang, X., Ma, Q., et al., Bioinspired drug-delivery system emulating the natural bone healing cascade for diabetic periodontal bone regeneration, *Bioact. Mater.*, 2023, vol. 21, pp. 324–339. https://doi.org/10.1016/j.bioactmat.2022.08.029
10. Kerry, R.G., Singh, K.R., Mahari, S., et al., Bioactive potential of morin loaded mesoporous silica nanoparti-

cles: A nobel and efficient antioxidant, antidiabetic and biocompatible abilities in in-silico, in-vitro, and in-vivo models, *OpenNano*, 2023, vol. 10, p. 100126. https://doi.org/10.1016/j.onano.2023.100126

11. Rivera, D. and Harris, J.M., In situ ATR-FT-IR kinetic studies of molecular transport and surface binding in thin sol–gel films: Reactions of chlorosilane reagents in porous silica materials, *Anal. Chem.*, 2001, vol. 73, no. 3, pp. 411–423. https://doi.org/10.1021/ac000947j
12. McCain, K.S., Schluesche, P., and Harris, J.M., Poly(amidoamine) dendrimers as nanoscale diffusion probes in sol–gel films investigated by total internal reflection fluorescence spectroscopy, *Anal. Chem.*, 2004, vol. 76, no. 4, pp. 939–946. https://doi.org/10.1021/ac0351015
13. McCain, K.S. and Harris, J.M., Total internal reflection fluorescence-correlation spectroscopy study of molecular transport in thin sol–gel films, *Anal. Chem.*, 2003, vol. 75, no. 14, pp. 3616–3624. https://doi.org/10.1021/ac0207731
14. McCain, K.S., Hanley, D.C., and Harris, J.M., Single-molecule fluorescence trajectories for investigating molecular transport in thin silica sol–gel films, *Anal. Chem.*, 2003, vol. 75, no. 17, pp. 4351–4359. https://doi.org/10.1021/ac0345289
15. Johnson, S.A., Olivier, P.J., and Mallouk, T.E., Ordered mesoporous polymers of tunable pore size from colloidal silica templates, *Science*, 1999, vol. 283, no. 5404, pp. 963–965. https://doi.org/10.1126/science.283.5404.96
16. Masalov, V.M., Dolganov, P.V., Sukhinina, N.S., et al., Synthesis of polymer-based inverted opal and transformation of its optical properties, *Adv. Nano Research*, 2014, vol. 2, no. 1, pp. 69–76. https://doi.org/10.12989/anr.2014.2.1.069
17. Lei, Z., Xiao, Y., Dang, L., et al., Fabrication of ultra-large mesoporous carbon with tunable pore size by monodisperse silica particles derived from seed growth process, *Microporous Mesoporous Mater.*, 2006, vol. 96, nos. 1–3, pp. 127–134. https://doi.org/10.1016/j.micromeso.2006.06.031
18. Sukhinina, N.S., Masalov, V.M., Zhokhov, A.A., et al., Synthesis and modification of carbon inverse opal nanostructres based on anthracene and their electrochemical characteristics, *Nanotechnol. Russ.*, 2017, vol. 12, nos. 11–12, pp. 635–642. https://doi.org/10.1134/S199507801706012X
19. Zakhidov, A.A., Baughman, R.H., Iqbal, Z., et al., Carbon structures with three-dimensional periodicity at optical wavelengths, *Science*, 1998, vol. 282, no. 5390, pp. 897–901. https://doi.org/10.1126/science.282.5390.897
20. Dai, B., Shu, G., Ralchenko, V., et al., 2D inverse periodic opal structures in single crystal diamond with incorporated silicon-vacancy color centers, *Diamond Relat. Mater.*, 2017, vol. 73, pp. 204–209. https://doi.org/10.1016/J.DIAMOND.2016.09.022
21. Kolbe, G., Das komplexchemiche Verhalten der Kieselsaure, *Dissertation*, Jena: Friedrich-Schiller Universitat, 1956.
22. Stöber, W., Fink, A., and Bohn, E., Controlled growth of monodisperse silica spheres in the micron size range, *J. Colloid Interface Sci.*, 1968, vol. 26, no. 1, pp. 62–69. https://doi.org/10.1016/0021-9797(68)90272-5
23. Bogush, G.A., Tracy, M.A., and Zukovski IV, C.F., Preparation of monodisperse silica particles: Control of size and mass fraction, *J. Non-Cryst. Solids*, 1988, vol. 104, no. 1, pp. 95–106. https://doi.org/10.1016/0022-3093(88)90187-1
24. Giesche, H., Synthesis of monodispersed silica powders I. Particle properties and reaction kinetics, *J. Eur. Ceram. Soc.*, 1994, vol. 14, no. 3, pp. 189–204. https://doi.org/10.1016/0955-2219(94)90087-6
25. Chang, S.M., Lee, M., and Kim, W.-S., Preparation of large monodispersed spherical silica particles using seed particle growth, *J. Colloid Interface Sci.*, 2005, vol. 286, no. 2, pp. 536–542. https://doi.org/10.1016/j.jcis.2005.01.059
26. van Helden, A.K., Jansen, J.W., and Vrij, A., Preparation and characterization of spherical monodisperse silica dispersions in nonaqueous solvents, *J. Colloid Interface Sci.*, 1981, vol. 81, no. 2, pp. 354–368. https://doi.org/10.1016/0021-9797(81)90417-3
27. Makrides, A.C., Turner, M., and Slaughter, J., Condensation of silica from supersaturated silicic acid solutions, *J. Colloid Interface Sci.*, 1980, vol. 73, no. 2, pp. 345–367. https://doi.org/10.1016/0021-9797(80)90081-8
28. Bailey, J.K. and Meckartney, M.L., Formation of colloidal silica particles from alkoxides, *Colloids Surf.*, 1992, vol. 63, nos. 1–2, pp. 151–161. https://doi.org/10.1016/0166-6622(92)80081-C
29. van Blaaderen, A., van Geest, J., and Vrij, A., Monodisperse colloidal silica spheres from tetraalkoxysilanes: Particle formation and growth mechanism, *J. Colloid Interface Sci.*, 1992, vol. 154, no. 2, pp. 481–501. https://doi.org/10.1016/0021-9797(92)90163-G
30. Chen, S.-L., Preparation of monosize silica spheres and their crystalline stack, *Colloids Surf.*, A, 1998, vol. 142, no. 1, pp. 59–63. https://doi.org/10.1016/S0927-7757(98)00276-3
31. Yokoi, T., Sakomoto, Y., Terasaki, O., et al., Periodic arrangement of silica nanospheres assisted by amino acids, *J. Am. Chem. Soc.*, 2006, vol. 128, no. 42, pp. 13664–13665. https://doi.org/10.1021/ja065071y
32. Davis, T.M., Snyder, M.A., Krohn, J.E., and Tsapatsis, M., Nanoparticles in lysine–silica sols, *Chem. Mater.*, 2006, vol. 18, no. 25, pp. 5814–5816. https://doi.org/10.1021/cm061982v
33. Hartlen, K.D., Athanasopoulos, A.P.T., and Kitaev, V., Facile preparation of highly monodisperse small silica spheres (15 to >200 nm) suitable for colloidal templating and formation of ordered arrays, *Lang-*

muir, 2008, vol. 24, no. 5, pp. 1714–1720. https://doi.org/10.1021/la7025285

34. Samarov, E.N., Mokrushin, A.D., Masalov, V.M., et al., Structural modification of synthetic opals during thermal treatment, *Phys. Solid State*, 2006, vol. 48, no. 7, pp. 1280–1283. https://doi.org/10.1134/S1063783406070109
35. Matsoukas, T. and Gulari, E., Dynamics of growth of silica particles from ammonia-catalyzed hydrolysis of tetra-ethyl-orthosilicate, *J. Colloid Interface Sci.*, 1988, vol. 124, no. 1, pp. 252–261. https://doi.org/10.1016/0021-9797(88)90346-3
36. Matsoukas, T. and Gulari, E., Monomer-addition growth with a slow initiation step: A growth model for silica particles from alkoxides, *J. Colloid Interface Sci.*, 1989, vol. 132, no. 1, pp. 13–21. https://doi.org/10.1016/0021-9797(89)90210-5
37. Chen, Sh.-L., Kinetics of formation of monodisperse colloidal silica particles through the hydrolysis and condensation of tetraethylorthosilicate, *Ind. Eng. Chem. Res.*, 1996, vol. 35, no. 12, pp. 4487–4493. https://doi.org/10.1021/ie9602217
38. Ratnikov, V.V., Determining the porosity of synthetic opals and porous silicon by X-ray methods, *Phys. Solid State*, 1997, vol. 39, no. 5, pp. 856–858. https://doi.org/10.1134/1.1129984

Translated by A. Kirilin